Marine Pollution Bulletin 114 (2017) 871–880

Contents lists available at ScienceDirect

Marine Pollution Bulletin

journal homepage: www.elsevier.com/locate/marpolbul

Settling velocity of microplastic particles of regular shapes

Liliya Khatmullina [a,b], Igor Isachenko [a,*]

[a] Atlantic Branch of P.P. Shirshov Institute of Oceanology of Russian Academy of Sciences, Prospect Mira, 1, Kaliningrad, 236022, Russia
[b] Immanuel Kant Baltic Federal University, A. Nevskogo street, 14, Kaliningrad, 236016, Russia

ARTICLE INFO

Article history:
Received 17 July 2016
Received in revised form 9 November 2016
Accepted 10 November 2016
Available online 15 November 2016

Keywords:
Microplastics
Regular shape
Settling experiment
Theoretical predictions of settling velocity

ABSTRACT

Terminal settling velocity of around 600 microplastic particles, ranging from 0.5 to 5 mm, of three regular shapes was measured in a series of sink experiments: Polycaprolactone (material density 1131 kg m^{-3}) spheres and short cylinders with equal dimensions, and long cylinders cut from fishing lines (1130–1168 kg m^{-3}) of different diameters (0.15–0.71 mm). Settling velocities ranging from 5 to 127 mm s^{-1} were compared with several semi-empirical predictions developed for natural sediments showing reasonable consistency with observations except for the case of long cylinders, for which the new approximation is proposed. The effect of particle's shape on its settling velocity is highlighted, indicating the need of further experiments with real marine microplastics of different shapes and the necessity of the development of reasonable parameterization of microplastics settling for proper modeling of their transport in the water column.

1. Introduction

In the last decade microplastics (MPs) became one of the major concerns in the scope of marine sciences. MPs are usually defined as small polymer particles with size <5 mm (Arthur et al., 2009). The lower limit varies between studies (Law and Thompson, 2014; Thompson, 2015; Ryan, 2015), being related to the sampling and processing methods (Hidalgo-Ruz et al., 2012). Physical properties of MPs found in the marine environment (such as density, shape, or surface texture) may vary significantly depending on the polymer's properties and duration of its exposure in the environment (Moret-Ferguson et al., 2010; Hidalgo-Ruz et al., 2012). MPs come into the environment as a result of a direct release (primary MPs) or from degradation/destruction of larger plastic debris (secondary MPs). The former typically have more or less regular shapes (like beads or spherules), while the latter may exhibit diverse shapes and arbitrary proportions. Thus, common shapes of MPs reported from sampling in marine environments are pellets, fibers, films, flakes, and fragments of various geometries (Carpenter et al., 1972; Hidalgo-Ruz et al., 2012; Woodall et al., 2014; Noik and Tuah, 2015; Esiukova, 2016).

Up to date, despite exponentially increasing number of studies on MPs in marine environment (Barboza and Gimenez, 2015), physical and dynamical properties of the very particles are poorly investigated. In particular, this applies to the terminal settling velocity, which is the characteristic feature of any negatively buoyant particle sedimenting in the water. The settling velocity is a valuable parameter for numerical simulation of microplastic debris transport pathways (Ballent et al., 2013; Critchell and Lambrechts, 2016), order-of-magnitude ecological estimates and theoretical description of general behavior of non-buoyant plastic particles in the water (Chubarenko et al., 2016).

In spite of that, only very few studies have concerned settling velocity of microplastics. Ballent et al. (2013) measured mean settling velocity and resuspension characteristics of beach high density (HD) black pellets of about 5 mm size. Measurements were conducted in saltwater with density close to that of seawater in the Nazaré Canyon of Portugal, since the research was focused on the numerical simulation of benthic microplastics transport in that area. Kowalski et al. (2016) conducted sinking experiments with particles of diverse polymer type, density, size, and shape in deionized water and natural seawater. The particles of irregular shape were used, produced by authors by comminuting virgin plastic pellets.

At the same time, the settling velocity is quite well investigated in the problems of hydrodynamics and sedimentology, both theoretically and experimentally. Being one of the key variables in the processes of suspension, sedimentation, and sediment transport, it has been subject to many sedimentological studies (Zanke, 1977; Hallermeier, 1981; Dietrich, 1982; Zhang, 1989; Julien, 1995; Soulsby, 1997; Cheng, 1997; Ahrens, 2000; Jiménez and Madsen, 2003; She et al., 2005; Wu and Wang, 2006) reviewed by Zhiyao et al. (2008) and Sadat-Helbar et al. (2009). Following these studies, the terminal settling velocity, w_s, is defined as the velocity of uniform motion or motion without acceleration. Thus, relatively small particle sinking in liquid achieves the terminal

* Corresponding author.
E-mail addresses: liliakhatmullina@gmail.com (L. Khatmullina), isatchenko@gmail.com (I. Isachenko).

http://dx.doi.org/10.1016/j.marpolbul.2016.11.024
0025-326X/

settling velocity when the hydrodynamical drag force and the gravitational forces are balanced, on the assumption that no other forces are acting on the particle in vertical direction (Allen, 1985):

$$\frac{1}{2}C_D\rho S w_s^2 = (\rho_s - \rho)gV \quad (1)$$

where C_D denotes the drag coefficient; S and V – the projected area and volume of the particle; ρ and ρ_s – the fluid and particle density, respectively; g – acceleration due to gravity.

The key issue here is to find an appropriate definition of the drag coefficient, C_D, of a particle (Dietrich, 1982), which depends, among others, on the Reynolds number defined as.

$$Re = w_s d/\nu, \quad (2)$$

where d is the characteristic length scale of a particle, and ν is the kinematic viscosity of the fluid. The Reynolds number characterizes the regime of the flow around the particle (White, 1999): laminar regime at $Re < 1$, turbulent regime at $10^3 < Re < 10^5$, and the transitional regime in-between (at $1 < Re < 10^3$).

Some analytical solutions were proposed for C_D at very low Re numbers in laminar regime (Stokes, 1851) and in turbulent regime (Dallavalle, 1948; Schlichting, 1979), but they are not applicable in-between – in transitional regime; analytical solution for the C_D in the full range of Re numbers is still absent. However, sedimentation of the majority of natural particles refers to the transitional flow. To cope with this problem, various semi-empirical formulae were proposed (e.g., Dietrich, 1982; Cheng, 1997; Ahrens, 2000; Camenen, 2007; Zhiyao et al., 2008). Motion of MPs in the ocean also falls in transitional flow regime (Chubarenko et al., 2016). The authors are not aware of any studies dedicated to testing predictions developed for natural sediment particles with MPs' settling, nor to the proposition of new settling velocity formulae designed specifically for microplastic particles.

It is well known (Dietrich, 1982) that, given the same volume and density, ideally round particles with smooth surface experience smaller drag and thus have larger sinking velocity, as compared to their angular counterparts. For natural sediment particles, influence of the particle shape on its settling velocity is considered in several studies (Dietrich, 1982; Jiménez and Madsen, 2003; Hazzab et al., 2008; Terfous et al., 2013). For irregularly shaped microplastic particles, Kowalski et al. (2016) revealed a noticeable deviation between their measured sinking velocity and that theoretically predicted (Dietrich, 1982) for perfect spheres of the same equivalent diameter. Both MPs and natural sediment particles vary in shapes and can be very irregular. Additionally, MPs may have specific geometries, including flat flakes and flexible fibers. Thus, accounting for the MPs shape is the highest priority problem.

In this study, we use our experimental data to test how far the settling velocity of non-buoyant MPs of regular (but not ideal) shapes deviates from that predicted by existing semi-empirical formulae developed for the natural and artificial grains (Jayaweera and Cottis, 1969; Dietrich, 1982; Julien, 1995; Soulsby, 1997; Cheng, 1997; Zanke, 1977; Zhang, 1989; Ahrens, 2000; Guo, 2002; Camenen, 2007; Zhiyao et al., 2008). We perform joint analysis of our data for the set of step-by-step changing shapes – from smooth quasi-spherical Polycaprolactone particles to semi-angular short cylinders and long cuts of fishing lines (FL cuts). We also demonstrate sensitivity of the settling behavior to these variations in shape and the scale of the velocity deviation due to shape irregularity, induced by fabrication process of Polycaprolactone particles and weathered FL cuts. Finally, we suggest a new prediction formula for the settling velocity of FL cuts with different diameters of 0.15–0.71 mm and lengths of 0.5–5 mm taken for MPs. The results are useful for understanding of basic physical behavior of MPs of the considered shapes in the marine environments, as well as for order-of-magnitude estimates of their settling velocities in natural waters and for numerical modeling of MPs transport. Our study suggests such investigations for other MPs shapes in future.

2. Materials, methods and theoretical background

2.1. The particles

Three groups of artificially made plastic particles (digital photographs are shown in Fig. 1) were analyzed in this study: spherical granules and cylinder-shaped granules hand-fabricated from Polycaprolactone plastic (PCL, material density 1131 kg m^{-3}), and pieces of aged fishing lines (FL) of different diameters and densities (0.15–0.71 mm, 1130–1168 kg m^{-3}) cut from the shreds found at the coastline. Choice of the particles was defined by several reasons. Spherical and cylindrical shapes are relatively abundant among the MPs found in the marine environments (Carpenter et al., 1972; Colton et al., 1974; Turner and Holmes, 2011; Noik and Tuah, 2015). On the other hand, settling velocity of idealized spheres (Cheng, 1997; Camenen, 2007; Sadat-Helbar et al., 2009; Terfous et al., 2013) and cylinders (Clift et al., 1978; Komar, 1980; Jianzhong et al., 2003; Gabito and Tsouris, 2008) is well-studied. The preparation procedure in case of spherical and cylinder-shaped PCL particles and exposure to the natural environments in case of pieces of fishing lines causes the irregularity of shape of the obtained particles. This allows to estimate how significantly shape influences the settling velocity, and to evaluate the applicability of the utilized settling velocity predictions in spite of the shape irregularities, characteristic to the real MPs.

Polycaprolactone (PCL) is the material, which is easy to handle as it softens during heating (up to 60 °C) and stiffens at room temperature, thus allowing the authors to produce particles of different shapes and sizes. Spherical particles were rolled from warm pieces of PCL. Cylinder-shaped granules were cut from circular rods of PCL with diameters ranging from 0.5 to 5 mm in such a way that the length (L) of resulting

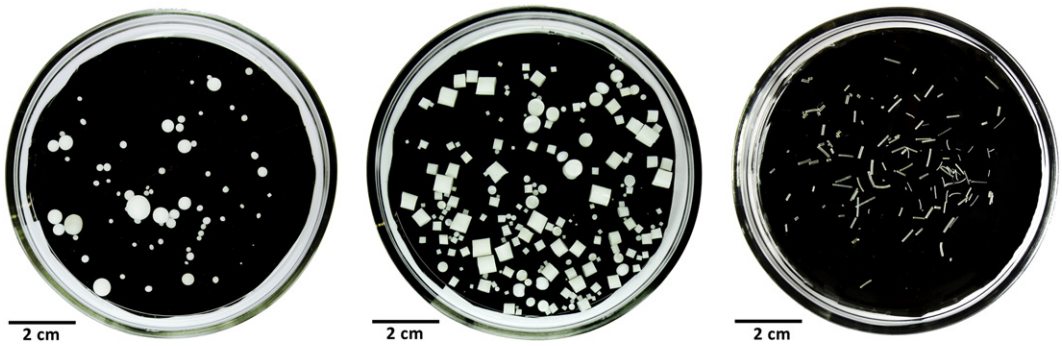

Fig. 1. Digital photographs of experimental particles. Particles are placed in the Petri dishes on the black background: left – Polycaprolactone (PCL) spheres, diameter 0.5–5 mm; center – PCL cylinders, cut from circular rods with diameters ranging from 0.5 to 5 mm in such a way that the length of resulting cylinder is approximately equal to its diameter, giving length to diameter ratio of around unity; right – fishing lines (FL) of different diameters cut into 0.5–5 mm long cylinders (FL cuts).

Table 1
Characteristics of experimental particles and water during the experiments. N denotes number of particles. For PCL spheres and cylinders "Diameter" implies nominal diameter, calculated as the diameter of a sphere with the same volume as the particle. Row "Diameter" consists of the ranges of nominal diameters of PCL spheres and PCL cylinders and diameters of fishing lines shreds, from which 6 sets of FL cuts were prepared, measurement inaccuracy was ±0.02 mm. The particle density, ρ_s is quoted as mean ± confidence interval 95%. Deviation of the water temperature, T during the experiments with each set of particles was no more than ±0.5°. The values for the fluid density, ρ at the measured water temperature were taken from Nikolsky (1966). The mean value of *L*/*D* ratio for PCL cylinders was 0.95 with standard deviation of 0.11.

	PCL spheres	PCL cylinders	FL cuts					
N	65	230	42	43	33	44	113	25
Diameter, mm	0.90–4.90	0.59–6.23	0.15	0.22	0.34	0.46	0.60	0.71
ρ_s, kg·m^{-3}	1131 ± 5.0	1131 ± 5.0	1135 ± 3.0	1156 ± 4.0	1168 ± 1.0	1146 ± 3.0	1130 ± 7.0	1148 ± 2.0
T, °C	25	26	26	26	22	26	26	22
ρ, kg·m^{-3}	997.0	996.8	996.8	996.8	997.8	996.8	996.8	997.8
L/*D*	undefined	0.6–1.26	1–37					

cylinder was equal to its diameter (*D*), giving length to diameter ratio of around unity (Table 1). In the following the abbreviations "PCL spheres" and "PCL cylinders" are used for simplification. Six shreds of fishing lines (with diameters of 0.15, 0.22, 0.34, 0.46, 0.60, and 0.71 mm) each long enough to produce a set of particles with different lengths were cut into pieces of 0.5–5 mm, which were abbreviated as fishing lines cuts or "FL cuts". Some shreds had marks of biofouling and surface contamination, which, as suggested by Morét-Ferguson et al. (2010), could increase the material density. However, as analyzing the effect of biofouling on the plastic density and its settling behavior itself represents a complex issue and requires different methodological approaches (e.g., Fazey and Ryan, 2016), it was out of the scope of this study. Thus, fishing line shreds were cleaned with alcohol before the FL cuts preparation and density measurements. In such a way, six sets of FL cuts distinguished by diameter were obtained. As a set of FL cuts was produced from one shred, the degree of surface degradation among the particles in a set was the same.

Density determination of the particles was performed by the titration method modified from ISO 1183-1 (2012). Randomly sampled particles from each set (PCL spheres, PCL cylinders, six sets of FL cuts with different diameters) were measured by the following procedure and the average value was used as density of the corresponding particle set. Each particle was placed in a 50-ml glass vial with distilled water and agitated to release any air bubbles on the surface of the sample. After the specimen had fallen to the bottom of the vial, a small portion of concentrated solution of zinc chloride (~1700 kg m^3) was added from the burette. The liquid was stirred after each addition. It was considered that the particle reached neutral buoyancy, when it stayed suspended within the liquid at the level to which it is brought by stirring without moving up or down for at least 1 min. At this point, 1 ml of the resulting solution was delivered via an automatic pipette to a tared flask on an analytical balance to determine the density of the liquid mixture.

The following sizes of individual particles were measured with a digital caliper of ±0.02 mm accuracy right before the sink experiment (Table 1): (1) three diameters of PCL spheres at right angles to each other (*a*, *b*, *c*); (2) length (*L*) and diameter (*D*) of PCL cylinders and FL cuts. Nominal diameter (D_n, Inter-Agency Committee, 1957) that equals to the diameter of a sphere with the same volume as the particle, was used as a measure of particle size for PCL spheres and cylinders and calculated as $D_n = \sqrt[3]{abc}$ and $D_n = \sqrt[3]{\frac{3}{2}LD^2}$, respectively. Deviation of hand-fabricated PCL spheres from perfect sphericity was evaluated using Corey shape factor (*csf*, Corey, 1949), which represents one of the most commonly used parameters to estimate such deviation (Komar and Reimers, 1978; Smith and Cheung, 2003). Values of *csf* for PCL spheres were calculated directly following the definition (Corey, 1949):

$$csf = \frac{c}{\sqrt{ab}}, \tag{3}$$

where *a*, *b*, and *c* are the longest, intermediate, and shortest axes of the particle in three orthogonal planes, respectively. It was also calculated for PCL cylinders, which have only two dimensions, thus $b = c = \min(L, D)$.

Several theoretical approximations utilized in this study required estimation of the Powers roundness coefficient (*P*, Powers, 1953). By definition it is determined via visual comparison of particles to the standard table images and distinguishes particles into six classes (very angular, $P = 1$; angular, $P = 2$; …; well-rounded, $P = 6$). Thus, the PCL spheres were assigned $P = 6$, whereas estimation of *P* for PCL cylinders was not so apparent. For each particle class, Powers (1953) specified ranges of Wadell roundness (Wadell, 1932), which is defined as average radius of curvature of corners divided by the radius of the largest inscribed circle and usually measured for the particle projection of the maximum area. For PCL cylinders with $L = D$ this maximum projected area is square, which in our understanding implies vanishingly small curvature of corners, giving Wadell roundness less than the range accounted in Powers' class of very angular particles (0.12–0.17). Powers also stated that the concept of roundness could not be validly applicable to the no rounded particles (e.g., crystals, Powers, 1953). On the other hand, considering another projection of PCL cylinders, which represents a circle, they would have Wadell roundness of 1.0 and $P = 6$ as well-rounded particles. Due to this uncertainty, in the formulae requiring *P* roundness the value that gave minimum error between predicted and measured velocities was used. This value was found through the trial-and-error procedure with *P* varying from 1.0 to 6.0 with a 0.5 step.

Additionally, aspect ratio (*L*/*D*) as the usual measure of the particle shape for cylinders with length larger than diameter (Clift et al., 1978; Komar, 1980; Gabito and Tsouris, 2008) was calculated for PCL cylinders and FL cuts and shown in Table 1.

2.2. Experimental setup and settling velocity measurements

Settling velocity was determined in series of sink experiments conducted in a glass column with 10 mm wall thickness, a square cross-section of 18 × 18 cm (inner size), and a height of 110 cm (Fig. 2) analogously to the common procedure of settling velocity measurements described in e.g., Gibbs et al. (1971), Allen (1985), Hazzab et al. (2008), and Ballent et al. (2013). The tank was filled with distilled water. Water properties during the experiments are given in Table 1. Water temperature near the surface and at the bottom of the tank was measured 15 min before and right after each series of experiments with one set of particles as follows: mercury thermometer tied on a string was slowly pulled down to the tank bottom and then slowly taken out. Authors suppose that 15 min is enough for the disturbances caused by the movement of thermometer in the water column to be dissipated to the negligible level. According to these measurements the temperature variation during each experiment was no >1° (±0.5 °C). Corresponding values of distilled water density and kinematic viscosity were taken from Nikolsky (1966). Variations of water kinematic viscosity for the observed temperature variations (±0.5 °C) were within 1.01% (Nikolsky, 1966).

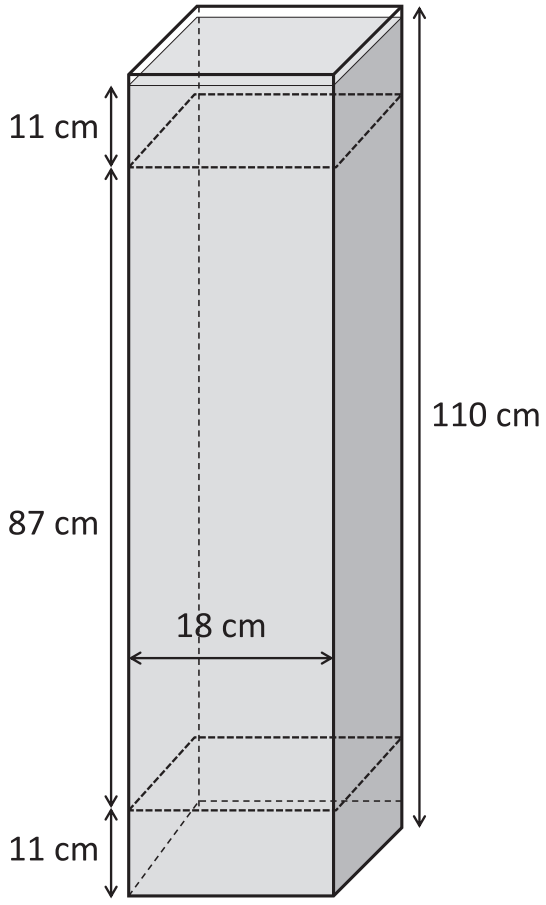

Fig. 2. Scheme of the experimental setup. Glass column of 110 cm height with a square cross-section of 18 × 18 cm, filled with distilled water. Marking lines, painted 11 cm below the water surface and 11 cm above the bottom are dashed. Resulting sinking distance is 87 cm.

Particles were placed approximately 1 cm below the water surface (so that the particles were not restrained by the surface tension) in the center of the tank by tweezers, and then let fall freely. The depth at which the particle achieved the terminal settling velocity was reached at around 10 cm. Thus, marking lines were painted over the tank sides 11 cm below the water surface, and 11 cm above the bottom. Finally, the time the particle took to cover 87 cm was measured with a stopwatch and the terminal settling velocity was calculated as the ratio of sinking distance to the duration of the fall.

2.3. Description of semi-empirical formulae utilized in the study

As the settling process of MPs relates to the transitional flow regime (according to the settling velocity estimations by Chubarenko et al. (2016), formulations developed specifically for the laminar or turbulent flow were not analyzed. Several semi-empirical formulae for perfect spheres (Dietrich, 1982) and natural sediment particles applicable in transitional flow regime (Dietrich, 1982; Julien, 1995; Soulsby, 1997; Cheng, 1997; Zanke, 1977; Zhang, 1989; Ahrens, 2000; Guo, 2002; Camenen, 2007; Zhiyao et al., 2008) were chosen for comparison with experimental data on PCL spheres and cylinders. Settling behavior of long cylinders and hence of the most of FL cuts differs from that of isometric (i.e. $L/D \approx 1$) cylinders and spheres and supposedly from the sediment particles. Therefore, an expression for non-isometric ($L/D > 1$) long cylinders (Jayaweera and Cottis, 1969, listed in Clift et al., 1978) was considered. Additionally, the approximation developed specifically for the FL cuts settling data was presented.

The ability of the implemented formulations to predict the settling velocities of experimental particles was estimated by calculating the coefficient of determination R^2 and the average value of the relative error, E, defined as follows (N – number of individual measurements):

$$E = \frac{1}{N}\sum_{i=1}^{N}\frac{(\text{predicted } w_s)_i}{(\text{experimental } w_s)_i} - 1.$$

The measurements and theoretical predictions were plotted in terms of dimensionless velocity (W_*) and dimensionless diameter (D_*) proposed by Dietrich (1982) and calculated as follows:

$$W_* = \frac{w_s^3}{g'\nu}, \tag{4}$$

$$D_* = \frac{g' D_n^3}{\nu^2}, \tag{5}$$

where D_n is nominal diameter of the particle, equal to the diameter of a sphere of the same volume as the particle (Inter-Agency Committee, 1957), and $g' = g\Delta\rho/\rho = g(\rho_s - \rho)/\rho$ is reduced gravity acceleration. Variations of particle density with temperature were neglected.

2.3.1. Settling velocity of spheres and natural sediments

A) Dietrich (1982) did a comprehensive work concerning the settling velocity of spherical and natural particles based on an extensive dataset, embracing a wide range of *Re* numbers and shapes. His approach had no explicit relation to the regime of the flow and represented an attempt to fit the data sets by the 4-order polynomial function, sequentially separating the effects of shape and roundness. Dietrich proposed three approximations which implement *csf* and *P* roundness coefficient: for perfect smooth spheres; for smooth, well-rounded particles of any shape; and for angular natural particles.

B) In another approach, the settling velocity of natural grains is predicted by formulating the drag coefficient in the wide range of *Re* numbers in one equation with two asymptotic solutions. It was implemented in different works (Sha, 1956; Zanke, 1977; Raudkivi, 1990) and generalized by Cheng (1997) in the following form:

$$C_D = \left[\left(\frac{A}{\mathrm{Re}}\right)^{1/m} + B^{1/m}\right]^m, \tag{6}$$

where A, B, and m denote empirical coefficients which account for the effect of shape and are calibrated using the experimental data. Such formulation implies that, depending on the *Re* number, the drag coefficient C_D approaches the Stokes solution ($C_D = A/Re$) when $Re \ll 1$ implying laminar regime of the flow, and approaches a constant value ($C_D = B$) with increasing *Re*, which is characteristic of the turbulent regime (Dallavalle, 1948; Schlichting, 1979). After substituting (6) into (1), with respect to *Re* definition given in (2), the settling velocity is expressed as

$$w_s = \frac{\nu}{d}\left[\sqrt{\frac{1}{4}\left(\frac{A}{B}\right)^{2/m} + \left(\frac{4}{3}\frac{D_*}{B}\right)^{1/m}} - \frac{1}{2}\left(\frac{A}{B}\right)^{1/m}\right]^m. \tag{7.1}$$

While implementing the same asymptotic approach described above, researchers determined these empirical A, B, and m coefficients in different ways. Zhiyao et al. (2008) deduced the drag coefficient equation from 19 studies in the notation which is idem or close to that

of the Cheng's formulation in Eq. (6), in order to compare the resulting A, B, and m coefficients and to propose their own settling velocity Eq. (7.2):

$$w_s = \frac{\nu}{d} D_*^3 \left[\left(\frac{3A}{4}\right)^{2/m} + \left(\frac{3B}{4} D_*^3\right)^{1/m} \right]^{-m/2}. \quad (7.2)$$

From the formulae reviewed by Zhiyao et al. (2008), only those developed for the natural sediments were chosen for the subsequent analysis in this study. These include 5 formulae for settling velocity by Zanke (1977), Zhang (1989), Julien (1995), Soulsby (1997), and Cheng (1997) presented in the notation of Eq. (7.1); and 2 formulae by Guo (2002) and Zhiyao et al. (2008) presented in the notation of Eq. (7.2) (corresponding A, B, m coefficients after Zhiyao et al. (2008), see Tables 1 and 2 on pages 39 and 40). Camenen (2007) noted that A, B, and m are not constants but rather complicated functions of shape and roundness, expressed by csf and P coefficient. Ahrens (2000) suggested another asymptotic solution for settling velocity, which was calibrated on natural sand grains and thus could account for the effects of angularity, without, however, defining the relation to the shape explicitly:

$$w_s = \frac{C_1 g' d^2}{\nu} + C_t \sqrt{g' d}, \quad (8)$$

where the first and the second terms are related to the laminar and turbulent flow regimes, respectively; C_1 and C_t denote the calibration coefficients.

The ability of the aforementioned formulations to predict the settling velocities of PCL particles was evaluated. Please note that settling rates of PCL spheres were compared with Dietrich (1982) and Camenen (2007) predictions for perfect spheres, given $csf = 1$ and $P = 6.0$. Their formulae were also applied to PCL cylinders, given the most frequent value of $csf = 0.97$ and P roundness, which was found through the trial-and-error procedure described in the previous section.

2.3.2. Formulae for long cylindrical particles

Many researches (Jayaweera and Cottis, 1969; Clift et al., 1978; Haider and Levenspiel, 1989; Gabito and Tsouris, 2008) directed their efforts to the development of settling velocity equations for non-isometric ($L/D > 1$) cylindrical particles. In this study, the explicit expression given in Clift et al. (1978, p.155, Table 6.1) that approximates the curves of Jayaweera and Cottis (1969) was used. This expression accounts for density, diameter, and length of the cylinders and is valid for the particles with $L/D > 1$ and $10^{-1} \le Re_D \le 10^2$ (where $Re_D = w_s D/\nu$) and $L/D > 1$.

We also made an attempt to derive a new approximation of experimental settling velocity of FL cuts based on the fact of linear dependence of $C_D Re_L$ composition on the particle length. The approach is fairly simple and straightforward. As far as the particles are oriented horizontally during the fall, the cross-sectional area approximately equals LD. Substituting this and the cylinder volume, $V = (\pi/4)LD^2$, into the Eq. (1), one obtains the following expressions for the drag coefficient and terminal settling velocity:

$$C_D = \frac{\pi}{2} \frac{1}{w_s^2} g' D, \quad (9)$$

and

$$w_s = \left[\frac{\pi}{2} \frac{1}{C_D} g' D \right]^{1/2}. \quad (10)$$

Surprisingly, Eq. (10) shows that w_s does not explicitly depend on L, although the experimental data obviously reveal such dependence. At the same time, the settling velocity is a function of the Re number (see Eq. (2)), where, by physical sense for the FL cuts, the characteristic length scale should be the particle length, L:

$$w_s = Re_L \nu / L.$$

Such definition of the Re number was also used by Komar (1980) while describing the settling velocity of circular cylinders in laminar regime.

Hence, it was supposed that w_s in Eq. (9) and C_D in Eq. (10) are implicit functions of length. Analysis of our experimental data suggests a linear dependence of the composition $C_D Re_L$ on the particle length, i.e.

$$C_D Re_L = c_1 L + c_2. \quad (11)$$

To keep the right-hand side of the Eq. (11) dimensionless, it is necessary to express c_1 in the inverse units of L, while c_2 is dimensionless. Substituting Eq. (11) and definition of Re_L number suitable for the long cylinders into Eq. (10), the settling velocity defines as.

$$w_s = \frac{\pi}{2} \frac{1}{\nu} g' \frac{DL}{c_1 L + c_2}. \quad (12)$$

3. Results and discussion

3.1. Settling velocity measurements

Results of around 600 measurements of settling velocity are given in Table 2. Experimental values ranged from 5 mm s^{-1} of the thinnest and shortest FL cut (0.5 mm length) to 127 mm s^{-1} of the biggest PCL sphere (4.9 mm diameter). Dependence of settling velocity on the particle size was observed in each particle set, while the character of this relationship was determined by shape and would be discussed in detail in the Section 3.3. Shape dependence. The obtained settling velocity range together with size varying from 0.5 to 5 mm and water kinematic viscosity of 1 mm^{-2} gives Reynolds numbers ranging in between 2.5 and 635. Thus, settling of experimental particles indeed relates to the transitional flow.

The considered groups of particles revealed different settling behavior during the experiments. In contrast to spherical PCL particles, various secondary movements like rotation, oscillation, and tumbling were observed for PCL cylinders. Additionally, during the fall, PCL cylinders did not always follow a rectilinear trajectory. As noticed by Becker (1959) and Hazzab et al. (2008), such movements occur when the Reynolds number associated with the diameter of the sphere having the same surface as the particle is above 200. This settling instability also implies greater drag force and lower settling velocity as compared to those of spherical particles (Dietrich, 1982; Hazzab et al., 2008).

FL cuts tended to fall with their long axis perpendicular to the direction of settling. The observed orientation of FL cuts is similar to that of glass cylinders with circular cross-section and lengths much greater than diameter, settling in glycerol (Komar, 1980). It is assumed that

Table 2
The measured settling velocity, mm·s^{-1}. Mean settling velocity is quoted with ± standard deviation. Column "Size" gives diameter ranges of PCL spheres and cylinders and diameters of 6 sets of FL cuts, which lengths in each set varied from 0.5 to 5 mm.

Particle sets	Size, mm	Mean	Min	Max
PCL spheres	0.90–4.90	59.7 ± 26.9	27.2	127.0
PCL cylinders	0.59–5.09	59.7 ± 20.8	13.7	97.1
FL cuts	0.15	6.7 ± 0.7	5	8.9
	0.22	9.6 ± 1.3	6.6	15.8
	0.34	13.2 ± 1.3	10.3	14.95
	0.46	19.2 ± 2	13.7	20.8
	0.60	23.6 ± 0.7	19.2	25.9
	0.71	24.6 ± 1.5	20.1	26.3

this kind of settling behavior is characteristic of any long cylindrical particles (Komar, 1980; Jayaweera and Mason, 1965; Jianzhong et al., 2003).

Shreds of fishing lines used for FL cuts preparation were initially winding, which reflects in slight curvature of experimental particles. For the longest FL cuts, it was noticed that they settle with the convex side directed downwards. In preliminary experiments it was observed that arched FL cuts took their stable horizontal orientation faster than the straight ones of the same length. Slow rotation of particles in horizontal plane, which is possibly caused by the curvature of the line, was also noticed during the sink experiments with FL cuts. Nevertheless, in this study, for the volume calculations and formula derivations, the curvature of the lines was considered negligible, assuming that all FL cuts were straight cylinders with measured L and D.

3.2. Comparison with theoretical predictions

Sinking velocities of PCL spheres were compared to Dietrich (1982) prediction for smooth spheres and Camenen (2007) formula (with $csf = 1$, $P = 6$) obtaining a good accordance ($E = 4.0\%$, $R^2 = 0.991$ and $E = 5.3\%$, $R^2 = 0.992$, respectively; Table 3, Fig. 3). At the same time, the calculated csf of PCL spheres was less than unity (csf range 0.8–1, Fig. 3) implying a slight deviation of their shape from a perfect spherical to ellipsoidal. This suggests applicability of these two formulae to predict settling of smooth well-rounded MP particles with shape close to spherical.

Dietrich (1982) approximation of naturally shaped grains and Camenen (2007) prediction, which both explicitly account for the particle shape and roundness via csf and P roundness coefficient, showed good agreement with the experimental settling rates of PCL cylinders. The least values of relative error equal to 7.4 and 5.4% were reached given $P = 3$ and $P = 5$ during the trial-and-error procedure for Dietrich's and Camenen's predictions, respectively. Noteworthy, Camenen (2007) inter alia calibrated his formula on the Dietrich's approximation and so it would be more logical if the roundness coefficients were identical. Therefore, although these two formulae have in general better predicting ability as they directly consider the effect of shape and show good accordance to the data, the uncertainty of roundness estimation reduces the applicability of these approaches. In respect to the MPs, whose shapes could be far from those of naturally occurring grains and/or have no rounded parts, it could be even more complicated to assign the correct P value, and there is a need either to test the existing methods (Wadell, 1932; Sneed and Folk, 1958) or to develop new approaches of roundness estimation specifically for MPs. Zhiyao et al. (2008) also noticed the complexity of Dietrich's and Camenen's formulae and the fact that Powers roundness coefficient is rarely measured in practice.

Table 3
Accuracy of fit of existing formulae against the experimental data on PCL particles.

Particle sets	Approximations	E	R^2
PCL spheres	Dietrich (1982)	4.0%	0.991
$N = 65$	Smooth spheres, $csf = 1$		
	Dietrich (1982)	20%	0.941
PCL cylinders	Smooth spheres, $csf = 1$		
$N = 438$	Dietrich (1982)	5.4%	0.961
	Angular particles, $csf = 0.97$, $P = 3.0$		
	Camenen (2007)	7.5%	0.949
	$csf = 0.97$, $P = 5.0$		
	Zanke (1977)[a]	11.7%	0.956
	Zhang (1989)[a]	10.2%	0.957
	Julien (1995)[a]	15.2%	0.956
	Soulsby (1997)[a]	10.4%	0.956
	Cheng (1997)[a]	14.5%	0.953
	Ahrens (2000)	6.6%	0.962
	Guo (2002)[a]	9.5%	0.956
	Zhiyao et al. (2008)	10.6%	0.958

N denotes the number of individual settling velocity measurements.
[a] Publications which were used in the comparative analysis by Zhiyao et al. (2008).

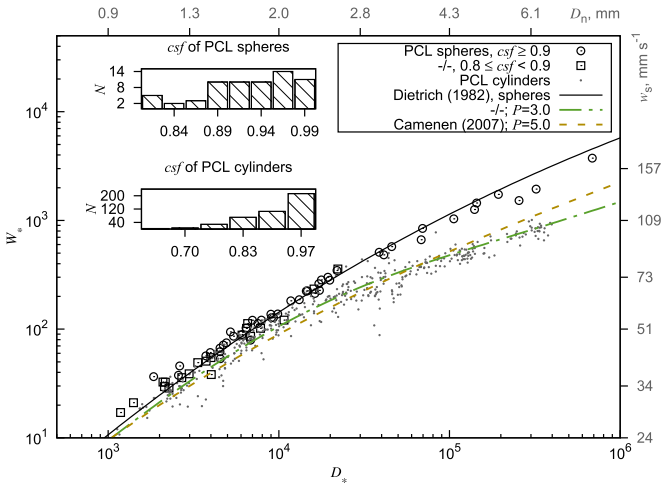

Fig. 3. Dimensionless settling velocity W_* and csf distribution of PCL spheres and cylinders. Corresponding dimensional axes are given, re-calculated for the example particle of $g' = 1300$ mm s^{-2} and $\nu = 1$ mm^2 s^{-1}. Open circles and squares denote experimental settling velocities of PCL spheres with $csf \geq 0.9$ and $0.8 \leq csf < 0.9$, respectively. Grey dots show experimental settling velocity of PCL cylinders. Solid line is a fourth order polynomial fit for smooth spheres, given by Dietrich (1982); dash-dot green line is Dietrich (1982) approximation for angular particles of any shape, $P = 3$, $csf = 0.97$; dashed yellow line represents Camenen (2007) prediction, $P = 5$, $csf = 0.97$.

In general, all the other settling velocity predictions used for comparison in this study (Fig. 4), where the shape is incorporated in a set of constant coefficients, were able to predict the experimental values of PCL cylinders settling with a good degree of consistency (within 14.5% of relative error, Table 3). Among them, the Ahrens (2000) curve, although it was calibrated on the data of Hallermeier (1981) in the quartz density range $1.58 < \Delta\rho/\rho < 1.67$, provided the best fit to data ($E = 6.6\%$, $R^2 = 0.962$; Table 3) when applied to PCL cylinders with $\Delta\rho/\rho = 1.13$. Finally, Ahrens' formula was considered as the most convenient to predict real MPs settling, in regard to the aforementioned inconsistency of P coefficient estimation.

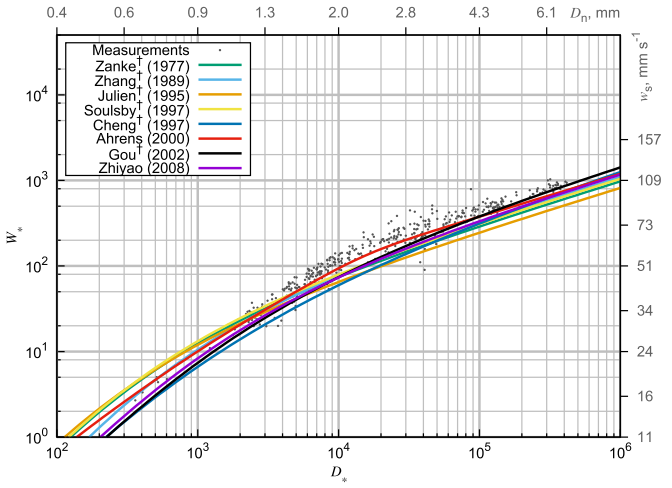

Fig. 4. Settling velocity of PCL cylinders versus particle diameter: experimental and predicted settling velocity in dimensionless form. Corresponding dimensional axes are given, re-calculated for the example particle of $g' = 1300$ mm s^{-2} and $\nu = 1$ mm^2 s^{-1}. Grey points denote experimental data; lines show the semi-empirical curves from different publications, colored according to the legend. † marks publications, which were used in comparative analysis by Zhiyao et al. (2008).

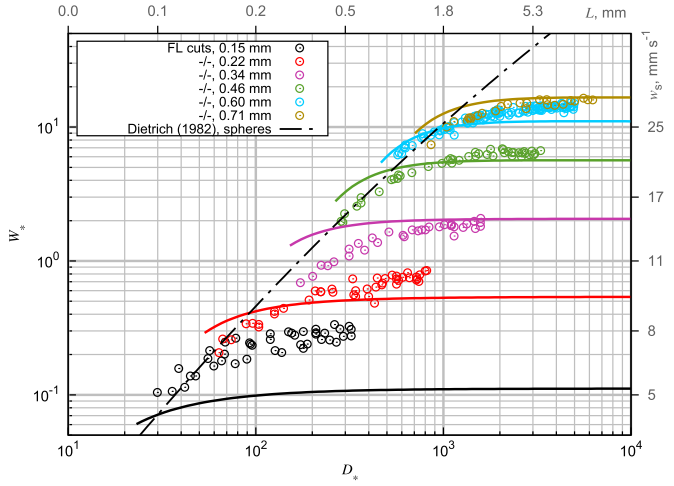

Fig. 5. Settling velocity of FL cuts in dimensionless form. Corresponding dimensional axes are given, re-calculated for the example FL cut of $g' = 1500$ mm s^{-2}, $D = 0.5$ mm, and $\nu = 1$ mm^2 s^{-1}. Open circles denote the experimental data. Dash-dot line – predicted settling velocity of smooth spheres (Dietrich, 1982). Solid lines – predicted settling velocity of cylinders with different diameters (Jayaweera and Cottis, 1969 as listed in Clift et al., 1978, p.155, Table 6.1). Colors correspond to the diameters of the FL cuts in accordance to the legend.

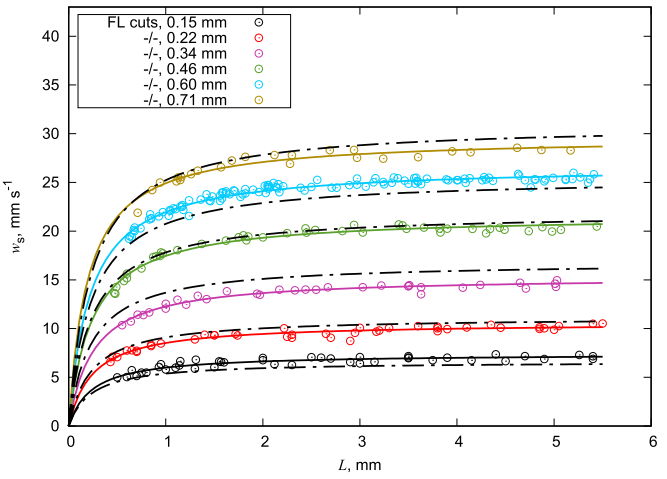

Fig. 7. Settling velocity of FL cuts of different diameters and the proposed approximations. Open circles denote the experimental data. Colored solid curves indicate settling velocity prediction by Eq. (12) for each set of FL cuts with different regression coefficients found by linear regressions of Eq. (11) to the individual data sets on FL cuts settling. Dash-dot black curves represent settling velocity predicted by Eq. (13) as a result of linear regression of all data points. The corresponding coefficients are given in Tables 4 and 5.

Fig. 5 shows that measured settling velocity of FL cuts does not resemble any of the semi-empirical curves for spherical or natural particles previously mentioned in the context of PCL particles settling (Dietrich (1982) approximation of smooth spheres is plotted for comparison). Mean settling rates of FL cuts are much lower than those of PCL spheres and cylinders (Table 2). Looking at the distribution of experimental points, we noticed that they fall into 6 distinct groups according to their diameter, which for convenience are shown in different colors in Figs. 5–7. The character of settling velocity dependence on the size of a particle in each set of FL cuts differs markedly from that of PCL spheres and cylinders. This relation was correctly described by Jayaweera and Cottis (1969). In our study, their empirical representation of terminal *Re* number (and therefore terminal settling velocity) as a function of *L*/*D* developed for long cylindrical particles was compared with settling rates of FL cuts. However, Jayaweera and Cottis (1969) curves were unable to predict the exact values with a good degree of consistency for thin FL cuts (E = 4.9–24.2%, R^2 = 0.972–0.810; Table 3).

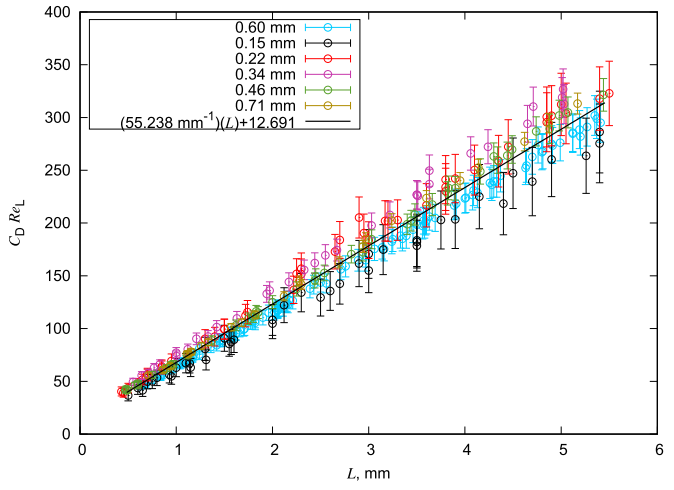

Fig. 6. The dependence of the product $C_D Re_L$ for FL cuts on their length. Circles with error bars denote the experimental data, colored according to the particle diameter. Black line is the linear approximation of all the experimental points, resulting regression coefficients are given in the legend.

Fig. 6 suggests that $C_D Re_L$ calculated using the measured settling velocity of FL cuts depends linearly on L. Calibration coefficients c_1 and c_2 were evaluated for each set of FL cuts by fitting Eq. (11) to the experimental data using the least squares algorithm (Table 4). According to the mean relative error, the resulting approximations show very good fit to the data (E = 1.1–3.7%, R^2 = 0.806–0.964) that confirms validity of Eq. (11) for each FL cuts set alone.

As the experimental points lie rather close to each other, a linear regression of all measured results was obtained and plotted on Fig. 6. It suggest the values of coefficients to be $c_1 = 55.238$ mm^{-1} and $c_2 = 12.691$. Final settling velocity formula takes the form:

$$w_s = \frac{\pi}{2}\frac{1}{\nu} g' \frac{DL}{55.238L + 12.691} \quad (mm\ s^{-2}) \tag{13}$$

It has a good approximation in the mean, but slightly overestimates or underestimates the w_s at the specific values of L (Fig. 7, dash-dot black curves). According to the values of mean relative error of Eq. (13) to the experimental data, the proposed formula mainly shows better performance than Jayaweera and Cottis (1969) prediction for each set of FL cuts. New formula reveals better feasibility (E = 6.0%, R^2 = 0.982) as compared to the one by Jayaweera and Cottis (1969) (E = 8.8%, R^2 = 0.972, Table 4) if applied to all the measurements on FL cuts settling. In general it could be concluded that FL cuts require a special approach.

Table 4
Regression coefficients c_1 and c_2 of Eq. (11), fitted to each set of FL cuts alone using the least squares algorithm and accuracy of fit of settling velocity prediction by Eq. (12) with the resulting coefficients to the experimental data.

Sets of FL cuts distinguished by diameter in mm	N	c_1, mm^{-1}	c_2	R^2	E
0.15	42	49.283	11.737	0.806	3.7%
0.22	43	58.282	14.179	0.917	2.4%
0.34	33	60.552	15.230	0.948	1.6%
0.46	44	55.985	13.334	0.964	1.8%
0.60	113	52.749	11.442	0.953	1.1%
0.71	25	57.726	11.058	0.910	1.4%

Table 5
Accuracy of fit of settling velocity prediction by Eq. (13) and Jayaweera and Cottis (1969) formula against the experimental data on FL cuts settling. Statistics is given for each set of FL cuts with equal diameter alone and for all measurement points.

Sets of FL cuts distinguished by diameter in mm	N	Eq. (13)		Jayaweera and Cottis (1969) as listed in Clift et al. (1978), p. 155, Table 6.1	
		R^2	E	R^2	E
0.15	42	0.807	10.1%	0.810	24.2%
0.22	43	0.917	6.5%	0.876	8.3%
0.34	33	0.949	10.9%	0.915	9.2%
0.46	44	0.965	2.3%	0.942	5.3%
0.60	113	0.953	5.0%	0.878	5.2%
0.71	25	0.906	2.7%	0.937	4.9%
All measurements	300	0.982	6.0%	0.972	8.8%

3.3. Shape dependence

Small PCL spheres with *csf* in the range 0.8–0.9 had settling velocities which corresponded well with the Dietrich (1982) approximation for perfect spheres ($E = 4.1\%$, $R^2 = 0.969$; Fig. 3). However, from Fig. 3 it could also be seen that settling velocities of large particles, which had relatively better spherical form as their *csf* ≥ 0.9, were slightly lower than those predicted by Dietrich curve. This is in accordance with several studies (Komar and Reimers, 1978; Jiménez and Madsen, 2003; Camenen, 2007; Hazzab et al., 2008) stating that the effect of shape is more pronounced for larger particles (i.e., higher *Re* numbers).

Analyzing Fig. 3, one can conclude that starting from approximately $D_* \approx 10^4$ ($W_* \approx 10^2$), which corresponds to $Re = (W_* D_*)^{1/3} \approx 100$, the settling velocity of angular PCL cylinders is noticeably lower than that predicted by Dietrich (1982) approximation for smooth spheres. This observation is in agreement with Dietrich (1982) stating that angularity of shape increases the drag and reduces the settling velocity for the same D_* as a sphere. The comparison also points out that the effect of shape becomes pronounced only after a certain size of a particle. Until it is relatively small, the settling of a particle does not deviate much from the settling of the corresponding sphere: settling rates of PCL cylinders deviate from those of PCL spheres at nominal diameter of around 2 mm. Emphasizing the difference between PCL spheres and cylinders, the Dietrich's prediction for smooth spheres shows the highest relative error of 20% when applied to the angular PCL cylinders, compared to 5.4–14.5% of other formulae (Table 3).

In respect to FL cuts, their settling rates have also demonstrated the influence of shape, which becomes pronounced with the increase in size (Fig. 5, Fig. 7). On the left (at smaller D_*, therefore smaller L), settling velocity of FL cuts begins with values which are close to the Dietrich (1982) approximation for smooth spheres. For larger D_*, the dependence of W_* on D_* (therefore on L) weakens and FL cuts exhibit settling velocity much lower than that of equivalent spheres. Such a shape of distribution can be explained as follows: (1) particles near the left-hand side have lesser values of L/D and hence are closer to the definition of isometric particles ($L \approx D$). And thus, their settling velocity is closer to that of spherical particles (2). When L (and hence L/D) increases, shape of FL cuts turns from isometric to elongated, and velocity increment decreases as the influence of end effects (Jayaweera and Mason, 1965; Komar, 1980) on the settling rates weakens, becoming negligible for the long cylinders ($L/D > 5$, in accordance with Jianzhong et al. (2003).

Fig. 8 gives an integrated evidence of a clear-cut distinction between the settling velocities of the particles considered in this study: the quasi-spherical particles (black solid curves), short isometric cylinders (red dash-dot curves) and the long cylinders (green dashed curves), as predicted by the formulae with the best fit to experimental data.

Thus, as Fig. 8 shows, the settling behavior of FL cuts markedly differs from that of spheres and cylinders starting from the smallest particles in the range, whereas settling rates of spheres and cylinders are quite similar. It could be also noticed that deviation between them increases with the increase in density access.

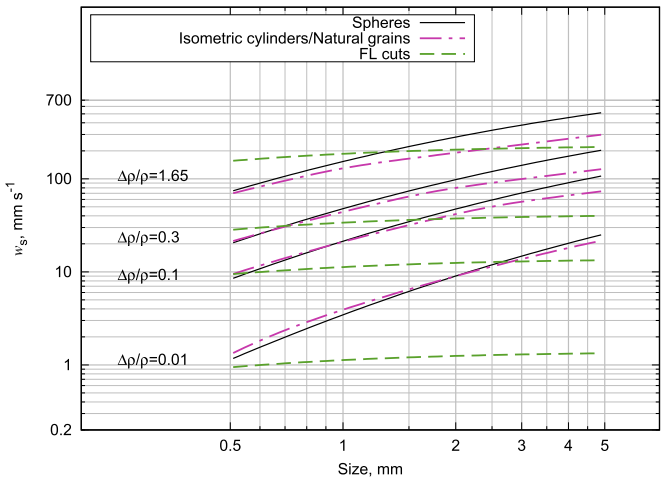

Fig. 8. Predicted settling velocities w_s of MPs particles of different sizes and relative excess densities $\Delta\rho/\rho$, in the range characteristic to MPs found in the marine environment. The excess densities were taken from Chubarenko et al. (2016). The size denotes the diameters of spheres and isometric cylinders or lengths of fishing lines cuts (for which 0.5 mm was taken as a diameter). Dietrich (1982) approximation of the perfect spheres is used for spherical particles (black solid line), Ahrens (2000) approximation of the natural grains – for short isometric cylindrical particles (red dash-dot line), and the new approximation presented in this study is used for the long cylinders (corresponding to FL cuts, green dashed line).

In a view of further numerical modeling of MPs transport, the approximations of perfect-spheres settling is credible for the particles with $Re < 100$, whereas, in general, we suggest that the dependence of settling behavior on the particle shape should be taken into account and parameterized in further modeling endeavors. Especially, when the shape of the particle by far deviates from that of naturally occurring grains, e.g. as the shape of some MPs, prediction of settling behavior requires much more effort and attention, and it definitely could not be parameterized by formulations of perfect spheres. This could be seen on example of FL cuts, for which we have suggested new approximation.

4. Conclusions

The aim of this study was to incorporate microplastics in the already existing body of marine sedimentology research. In the set of laboratory experiments with microplastic particles of simple regular shapes, we measured their settling velocities and compared them with several semi-empirical predictions, developed for natural sediments in a wide range of the *Re* numbers.

The leading effect of a MPs particle shape on its settling behavior is highlighted. The considered groups of particles – hand-made Polycaprolactone (PCL) spheres, short PCL cylinders and fishing line (FL) cuts – revealed different settling behaviors during the experiments. In contrast to spherical PCL particles, the PCL cylinders were rotating, oscillating, and tumbling during the fall. The FL cuts tended to settle with their long axis perpendicular to the direction of fall and this kind of settling behavior is characteristic of any long cylindrical particles.

Experimental values of the settling velocity of the used microplastic particles ranged from 5 mm s^{-1} for the thinnest and shortest FL cuts (0.5 mm length) to 127 mm s^{-1} of the largest PCL sphere (4.9 mm in diameter). The measured velocities were much different for different particle shapes. Dependence of settling velocity on the particle size was obvious for each particle set of a certain shape, while the character of this relation of the velocity from the size was pre-determined by the shape and could not be described by a single universal dependency. This way, the smallest prediction error was provided by the formulae specific for the particles of the particular shape. The effect of shape was more pronounced for larger particles (i.e., for higher *Re* numbers).

The results of our experiments are quite important for practical issues. It was our intension in this study to use not perfect shapes (of the PCL particles) and environmentally exposed surface texture (of fishing line cuts) to check the sensitivity of the existing analytical approximations to these "imperfections". Now, several practically useful conclusions can be deduced. Firstly, this is the general shape of the particle (spherical, cylindrical, elongated, etc.) which is of primary importance for its settling behavior: it prescribes the character of the motion and, thus, the corresponding semi-empirical dependency for the settling velocity. This provides certain logic to the analysis of motion of real marine MPs particles, which exhibit wide spectra of different physical properties. Secondly, an error of the predictions of the settling velocity of the MPs particles, initially developed for the corresponding basic shapes and natural sand particles, is within 10% only. Thus, the imperfections of the shape and the peculiarities of the surface texture, so characteristic of real marine microplastic particles, are able to cause deviations of the settling velocity, which are one order of magnitude smaller than the values predicted by already known formulae for the given general particle shape.

Future experimental work should give the priority to the estimation of the settling velocities of the real marine microplastics of other typical MPs shapes, in particular – fibers, films, and flat angular particles. Presumably, they would exhibit much more different settling behavior, showing various secondary movements during their free flight towards the eternal life in deep bottom sediments.

Acknowledgements

The authors acknowledge Dr. Sci. Irina Chubarenko for guidance and valuable comments on the paper drafts; Margarita Bagaeva for the language review; Dr. Mikhail Zobkov and Dr. Andrei Bagaev for fruitful discussions on the statistical analysis of the obtained results. Portions of this study were presented in abstract form at the EGU General Assembly 2016, Vienna, Austria 17–22 April 2016; MICRO 2016 Fate and impact of Microplastics in Marine Ecosystems, Lanzarote, Spain, 25–27 May 2016; and EMECS'11 SeaCoasts XXVI Joint Conference, Saint-Petersburg, Russia, 22–27 August 2016.

The study is supported by Russian Science Foundation via grant number 15-17-10020.

References

Ahrens, J.P., 2000. A fall-velocity equation. J. Waterw. Port Coast. Ocean Eng. 126, 99–102.
Allen, J.R.L., 1985. Sink or swim. In: Allen, Unwin (Eds.), Physical Sedimentology, pp. 39–54 (Chapter 3).
Arthur, C., Baker, J., Bamford, H., 2009. Proceedings of the International Research Workshop on the Occurrence, Effects and Fate of Micro-Plastic Marine Debris, September 9–11, 2008. NOAA Technical Memorandum NOS-OR&R-30 (49 p).
Ballent, A., Pando, S., Purser, A., Juliano, M.F., Thomsen, L., 2013. Modelled transport of benthic marine microplastic pollution in the Nazaré Canyon. Biogeosciences 10, 7957–7970.
Barboza, L.G.A., Gimenez, B.C.G., 2015. Microplastics in the marine environment: current trends and future perspectives. Mar. Pollut. Bull. 97, 5–12.
Becker, H.A., 1959. The effects of shape and Reynolds number on drag in the motion of a freely oriented body in an infinite fluid. Can. J. Chem. Eng. 37, 85–91.
Camenen, B., 2007. Simple and general formula for the settling velocity of particles. J. Hydraul. Eng.-ASCE 133, 229–233.
Carpenter, E.J., Anderson, S.J., Harvey, G.R., Miklas, H.P., Peck, B.B., 1972. Polystyrene spherules in coastal waters. Science 178, 749–750.
Cheng, N.S., 1997. Simplified settling velocity formula for sediment particle. J. Hydraul. Eng.-ASCE 123, 149–152.
Chubarenko, I., Bagaev, A., Zobkov, M., Esiukova, E., 2016. On some physical and dynamical properties of microplastic particles in marine environment. Mar. Pollut. Bull. 108, 105–112.
Clift, R., Grace, J.R., Weber, M.E., 1978. Nonspherical rigid particles at higher Reynolds numbers. Bubbles, Drops, and Particles. Academic Press, New York, pp. 142–168 (Chapter 6).
Colton, J.B., Knapp, F.D., Burns, B.R., 1974. Plastic particles in surface waters of the northwestern Atlantic. Science 185, 491–497.
Corey, A.T., 1949. Influence of Shape on the Fall Velocity of Sand Grains. (Master's Thesis). A&M College, Colorado .
Critchell, K., Lambrechts, J., 2016. Modelling accumulation of marine plastics in the coastal zone; what are the dominant physical processes? Estuar. Coast. Shelf Sci. 171, 111–122.
Dallavalle, J.M., 1948. Micrometrics: The Technology of Fine Particles. Pitman, London (555 p).
Dietrich, W.E., 1982. Settling velocity of natural particles. Water Resour. Res. 18, 1615–1626.
Esiukova, E., 2016. Plastic pollution on the Baltic beaches of Kaliningrad region, Russia. Mar. Pollut. Bull. 114, 1072–1080.
Fazey, F.M., Ryan, P.G., 2016. Biofouling on buoyant marine plastics: an experimental study into the effect of size on surface longevity. Environ. Pollut. 210, 354–360.
Gabito, J., Tsouris, C., 2008. Drag coefficient and settling velocity for particles of cylindrical shape. Powder Technol. 183, 314–322.
Gibbs, R.J., Matthews, M.D., Link, D.A., 1971. The relationship between sphere size and settling velocity. J. Sediment. Res. 41, 7–18.
Guo, J., 2002. Logarithmic matching and its applications in computational hydraulics and sediment transport. J. Hydraul. Res. 40, 555–565.
Haider, A., Levenspiel, O., 1989. Drag coefficient and terminal velocity of spherical and nonspherical particles. Powder Technol. 58, 63–70.
Hallermeier, R.J., 1981. Terminal settling velocity of commonly occurring sand grains. Sedimentology 28, 859–865.
Hazzab, A., Terfous, A., Ghenaim, A., 2008. Measurement and modeling of the settling velocity of isometric particles. Powder Technol. 184, 105–113.
Hidalgo-Ruz, V., Gutow, L., Thompson, R.C., Thiel, M., 2012. Microplastics in the marine environment: a review of the methods used for identification and quantification. Environ. Sci. Technol. 46, 3060–3075.
Inter-Agency Committee, 1957. Some Fundamentals of Particle Size Analysis: A Study of Methods Used in Measurement and Analysis of Sediment Loads in Streams. Rep. No. 12, Subcommittee on Sedimentation, Interagency Committee on Water Resources, St. Anthony Falls Hydraulic Laboratory, Minneapolis.
ISO 1183-1, 2012. Plastics – Methods for Determining the Density of Noncellular Plastics – Part 1: Immersion Method, Liquid Pyknometer Method and Titration Method. Geneva, Switzerland. pp. 1–17 (2012(E)).
Jayaweera, K.O.L.F., Cottis, R.E., 1969. Fall velocities of plate-like and columnar ice crystals. Q. J. R. Meteorol. Soc. 95, 703–709.
Jayaweera, K.O.L.F., Mason, B.J., 1965. The behaviour of freely falling cylinders and cones in a viscous fluid. J. Fluid Mech. 22, 709–720.
Jianzhong, L., Xing, S., Zhenjiang, Y., 2003. Effects of the aspect ratio on the sedimentation of a fiber in Newtonian fluids. J. Aerosol Sci. 34, 909–921.
Jiménez, J.A., Madsen, O.S., 2003. A simple formula to estimate settling velocity of natural sediments. J. Waterw. Port C-ASCE 129, 70–78.
Julien, Y.P., 1995. Erosion and Sedimentation. Cambridge University Press, Cambridge .
Komar, P.D., 1980. Settling velocities of circular cylinders at low Reynolds numbers. J. Geol. 88, 327–336.
Komar, P.D., Reimers, C.E., 1978. Grain shape effects on settling rates. J. Geol. 193–209.
Kowalski, N., Reichardt, A.M., Waniek, J.J., 2016. Sinking rates of microplastics and potential implications of their alteration by physical, biological, and chemical factors. Mar. Pollut. Bull. 109, 310–319.
Law, K.L., Thompson, R., 2014. Microplastics in the sea. Science 345, 144–145.
Reference book of chemist. In: Nikolsky, B.P. (Ed.), Moscow-Leningrad: Chemistry, second ed. vol. 1, p. 1070 (in Russian).
Morét-Ferguson, S., Law, K.L., Proskurowski, G., Murphy, E.K., Peacock, E.E., Reddy, C.M., 2010. The size, mass, and composition of plastic debris in the western North Atlantic Ocean. Mar. Pollut. Bull. 60, 1873–1878.
Noik, V.J., Tuah, P.M., 2015. A first survey on the abundance of plastics fragments and particles on two sandy beaches in Kuching, Sarawak, Malaysia. IOP Conference Series: Materials Science and Engineering vol. 78, No. 1. IOP Publishing, p. 012035.
Powers, M.C., 1953. A new roundness scale for sedimentary particles. J. Sediment. Res. 23.
Raudkivi, A.J., 1990. Loose Boundary Hydraulics. third ed. Pergamon Press, Inc., Tarrytown, N.Y.
Ryan, P.G., 2015. A brief history of marine litter research. In: Bergmann, M., Gutow, L., Klages, M. (Eds.), Marine Anthropogenic Litter. Springer, Berlin, pp. 1–25.
Sadat-Helbar, S.M., Amiri-Tokaldany, E., Darby, S., Shafaie, A., 2009. Fall velocity of sediment particles. Proceedings of the 4th IASME/WSEAS International Conference on Water Resources, Hydraulics and Hydrology, WHH'09.
Schlichting, H., 1979. Boundary Layer Theory. McGraw-Hill, New York (800 p).
Sha, Y.Q., 1956. Basic principles of sediment transport. J. Sediment. Res. 1, 1–54.
She, K., Trim, L., Pope, D., 2005. Fall velocities of natural sediment particles: a simple mathematical presentation of the fall velocity law. J. Hydraul. Res. 43, 189–195.
Smith, D.A., Cheung, K.F., 2003. Settling characteristics of calcareous sand. J. Hydraul. Eng. 129, 479–483.
Sneed, E.D., Folk, R.L., 1958. Pebbles in the lower Colorado River, Texas, a study in particle morphogenesis. J. Geol. 66, 114–150.
Soulsby, R.L., 1997. Dynamics of Marine Sands. Thomas Telford, London .
Stokes, G.G., 1851. On the Effect of the Internal Friction of Fluids on the Motion of Pendulums. vol. 9. Pitt Press.
Terfous, A., Hazzab, A., Ghenaim, A., 2013. Predicting the drag coefficient and settling velocity of spherical particles. Powder Technol. 239, 12–20.
Thompson, R.C., 2015. Microplastics in the marine environment: sources, consequences and solutions. In: Bergmann, M., Gutow, L., Klages, M. (Eds.), Marine Anthropogenic Litter. Springer, Berlin, pp. 185–200.
Turner, A., Holmes, L., 2011. Occurrence, distribution and characteristics of beached plastic production pellets on the island of Malta (central Mediterranean). Mar. Pollut. Bull. 62, 377–381.
Wadell, H., 1932. Volume, shape, and roundness of rock particles. J. Geol. 40, 443–451.
White, F.M., 1999. Fluid Mechanics. fourth ed. WCB/McGraw-Hill (225 p.).

Woodall, L.C., Sanchez-Vidal, A., Canals, M., Paterson, G.L., Coppock, R., Sleight, V., Calafat, A., Rogers, A.D., Narayanaswamy, B.E., Thompson, R.C., 2014. The deep sea is a major sink for microplastic debris. R. Soc. Open Sci. 1, 140317.

Wu, W., Wang, S.S.Y., 2006. Formulas for sediment porosity and settling velocity. J. Hydraul. Eng. 132, 858–862.

Zanke, U., 1977. Berechung der Sinkgeschwindigkeiten von sedimenten. Mitt. Des Franzius-Instituts fur Wasserbau. 46 p. 243.

Zhang, R.J., 1989. Sediment Dynamics in Rivers. Water Resources Press, Beijing (in Chinese).

Zhiyao, S., Tingting, W., Fumin, X., Ruijie, L., 2008. A simple formula for predicting settling velocity of sediment particles. Water Sci. Eng. 1, 37–43.